Imaging of microwave intermodulation fields in a superconducting microstrip resonator

Wensheng Hu,[a] A. S. Thanawalla, B. J. Feenstra,[b] F. C. Wellstood, and Steven M. Anlage[c]
Center for Superconductivity Research, Department of Physics, University of Maryland, College Park, Maryland 20742-4111

(Received 12 July 1999; accepted for publication 7 September 1999)

Nonlinearities give rise to intermodulation distortion in superconducting microwave devices and currently limit their use to low power applications. We have developed a cryogenic imaging technique to spatially resolve intermodulation distortion and used it to image an 8.2 GHz high temperature superconducting $Tl_2Ba_2CaCu_2O_8$ microwave resonator. The images reveal that the fundamental and intermodulation electric fields obey a fixed relation throughout the device. We note that further refinements of intermodulation theory in resonant devices may be required to fully describe the data. © *1999 American Institute of Physics.* [S0003-6951(99)04944-X]

The problem of nonlinearity currently restricts the use of high temperature superconductors to low power microwave applications. It is well known that the hole-doped cuprate superconductors have intrinsic nonlinearities due to their *d*-wave pairing-state symmetry.[1] However, practical thin film materials display microwave nonlinearities which are several orders of magnitude larger than those expected from intrinsic sources.[2] Extrinsic sources of nonlinearity include grain boundary weak links,[3] damage at patterned edges, heating,[4] and other phenomena.[5] The identification of these extrinsic sources is a first and essential step in eliminating them from materials used in microwave devices, and extending the range of applications of superconducting materials.

Nonlinearities fundamentally arise from a surface impedance $Z_s = R_s + iX_s$ which is dependent on the excitation level. Direct measurements of the nonlinear surface resistance (R_s) and reactance (X_s) in high temperature superconductors have shown a wide variety of behaviors, ranging from increases which are linear, quadratic, or stronger in radio-frequency (rf) magnetic field strength,[6] to surface impedance values which *decrease* over a substantial range of field strength before increasing.[7] At present there is no satisfactory microscopic explanation of these results, and this suggests that efforts be made to locally probe the nonlinear response of superconductors.

Measurements of harmonic generation have been widely used to characterize superconducting nonlinearities.[8,9] Here too there are a variety of results, explained by weak links and current crowding at the edges of the material. Probably the most sensitive experimental characterization of superconducting nonlinearity is through intermodulation distortion (IMD) of two nearby pure tones.[1,3,4] Intermodulation is also a practical measurement because it simulates the undesirable generation of ghost signals in a communication bandpass filter. We have chosen to focus our imaging efforts on IMD measurements because of their sensitivity and practicality.

As a first approach to localized imaging of nonlinear response, in this letter we describe a technique for spatially resolved imaging of intermodulation distortion in superconducting resonators. We image the electric fields at the fundamental and intermodulation frequencies in a practical high temperature superconducting microwave resonator as a function of temperature. Our experimental configuration is shown schematically in Fig. 1. The superconducting resonator under test is installed in a cryogenic scanning microwave microscope[10,11] and capacitively excited by a center conductor pin. Two microwave synthesizers send continuous wave (cw) tones at frequencies f_1 and f_2 into the device through isolators, amplifiers, and a combiner. The electric fields above the sample are detected through a scanned open-ended coaxial probe. We use a coaxial cable probe with a center conductor diameter $d_c = 200\,\mu$m and an outer diameter $d_o = 860\,\mu$m.[12] During a scan, the probe is held at a constant height above the sample, typically between 10 μm and several millimeters. The electric field above the sample induces a high-frequency potential difference between the center and grounded outer conductors of the probe. The probe is connected to a spectrum analyzer which can selectively measure the power at the linear response frequencies f_1 and f_2, or at the nearby third order IMD frequencies $2f_1 - f_2$ and $2f_2 - f_1$. We use a computer to record the response at these four

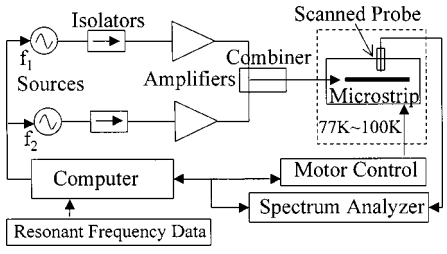

FIG. 1. Schematic of the microwave intermodulation experiment. The two sources provide signals to the device, while the scanned open-ended coaxial probe picks up the vertical component of the electric field. The collected power at different frequencies is selectively detected by the spectrum analyzer.

[a]Present address: Hughes Network Systems, 11717 Exploration Lane, Germantown, MD 20876.
[b]Present address: Philips Research Laboratories, Bldg. WB 1-09, Prof. Holstlaan 4, 5656 AA Eindhoven, The Netherlands.
[c]Electronic mail: anlage@squid.umd.edu

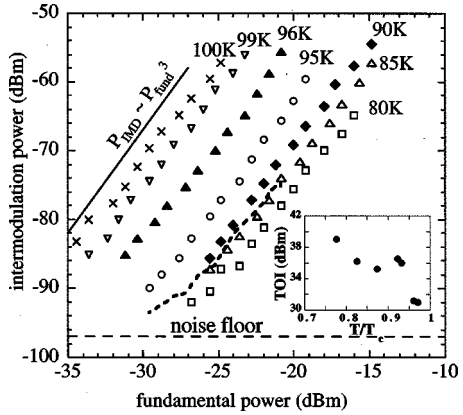

FIG. 2. Global intermodulation ($2f_1-f_2$) power measured at the open end of the microstrip at a height of 200 μm vs the measured power at the fundamental frequency $f_1=8.2$ GHz, at several temperatures. Also shown is 85 K data (dashed line) from the line cut of an image taken at a height of 200 μm, plotted in the same manner as the global data. The inset shows the third-order intercept (TOI) power in dBm vs reduced temperature T/T_c.

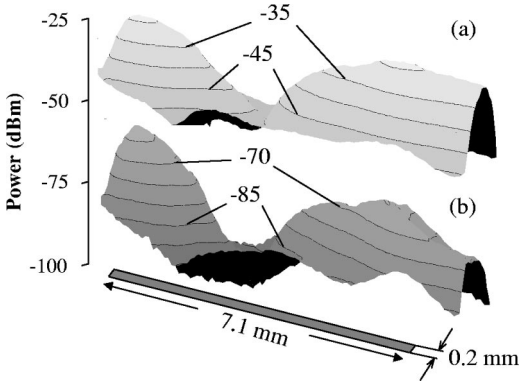

FIG. 3. Surface plots of (a) power at the fundamental frequency $f_1=8.2$ GHz of the superconducting resonator, and (b) intermodulation ($2f_1-f_2$) power, vs position over the microstrip resonator at 96 K. The approximate location of the microstrip is shown as the shaded rectangle and the drive pin is on the left side. The input power is +16 dBm for both tones and the height of the probe is 550 μm.

different frequencies and also control a two-axis translation stage, which raster scans the sample underneath the probe.

For realistic testing of this technique, we imaged a $Tl_2Ba_2CaCu_2O_8$ thin film microstrip resonator which was deposited on an MgO substrate. The microstrip has a T_c of 103 K and a fundamental resonant frequency at 77 K of approximately 8.2 GHz.[10] Figure 2 shows the results of standard ''global'' intermodulation measurements on this resonator as a function of temperature, measured using a probe which is positioned over the end of the resonator opposite the drive pin. The two tones are chosen to be 100 kHz apart to avoid the phase noise of the synthesizers at small frequency separations, and to remain within the middle of the passband of the resonator at 8.2 GHz ($Q\sim700-1400$, depending on temperature).

We see from Fig. 2 that the IMD power increases roughly as a power law of the incident microwave power. However, the power-law exponent is typically less than 3, whereas ideally one expects that third-order IMD power will always increase three times faster than the incident power.[13] This is because a third-order nonlinearity is the first nonzero term in the Taylor series expansion of the current–voltage ($I-V$) curve in time-reversal symmetric nonlinear systems. In practice, however, the situation is more complicated, and deviations are frequently seen.[14,15] Figure 2 also shows that IMD power grows as the transition temperature is approached from below (the inset shows that the approximate third-order intercept power decreases from +39 dBm at 80 K to +31 dBm at 99 K), indicating that nonlinearities grow stronger as the superfluid density diminishes.

We next imaged the microwave fields above the device while applying two cw tones at +16 dBm which were 100 kHz apart and centered on the fundamental resonant frequency. To accomplish this, we had to account for perturbations of the fundamental resonant frequency of the device due to the presence of the probe.[11] Consequently, we first scanned the region of interest, recording the resonant frequency of the microstrip as a function of the position of the probe. Then we scanned the same region again, using the resonant frequency data to align the two tones so that they were centered within the passband of the device at each probe location (Fig. 1). Figure 3 shows the resulting images of detected power versus position above the microstrip resonator at both the applied frequency f_1 and the intermodulation frequency $2f_1-f_2$. The f_1 image [Fig. 3(a)] is similar to our previous results on this resonator,[10] although the present image shows significantly greater dynamic range because of the use of a spectrum analyzer, rather than a diode, as a detector. The peak signals at either end of the resonator, and the minimum at the center, are consistent with a probe which detects power from just the z component of electric field in the fundamental standing wave pattern of this resonator.[10,12]

Figure 3(b) shows the intermodulation power versus position measured at the same time as the response at f_1. The IMD signal is smaller in amplitude but has a similar distribution in space. Upon closer inspection, however, one notes that the IMD image shows larger variations in power with position. This can be seen by taking longitudinal line cuts through the images in Fig. 3, as shown in Fig. 4. The response at f_1 fits qualitatively to a $\cos^2(\pi x/L)$ form, where x is the position along the resonator of length L, as expected for the fundamental standing wave.[16] In contrast, the intermodulation power is better fit to a $\cos^6(\pi x/L)$ form, showing that there is approximately a 3 to 1 ratio of IMD power to fundamental power point-by-point throughout the device.

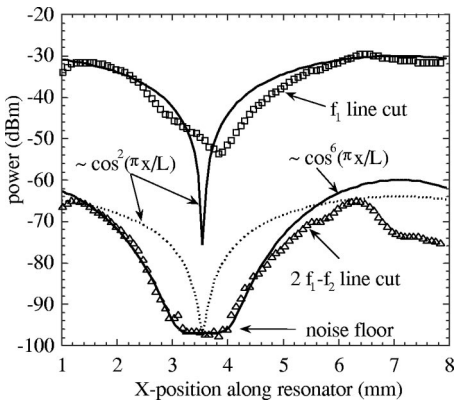

FIG. 4. Line cuts taken along the microstrip in Figs. 3(a) and (b). The resonator extends from $x=0$ to $x=L=7.1$ mm. Also shown are fits to $\cos^2(\pi x/L)$ (fundamental) and $\cos^6(\pi x/L)$ (IMD) forms.

Further insight into the distribution of IMD power in the resonator can be gained by plotting line cuts of fundamental and IMD images along side the global IMD data obtained by sweeping power. The dashed line and data points in Fig. 2 shows a comparison of these two entirely different methods of measuring IMD power at 85 K. The close agreement between these curves shows that the global IMD versus linear power information is present throughout the resonator. This suggests that information about local nonlinearities may be subsumed by the resonant nature of the IMD response.

The $\cos^6(\pi x/L)$ distribution of the IMD power is a well-known prediction of theories of intermodulation and third harmonic generation in superconducting resonators.[1,17] However, existing treatments make the approximation that the IMD electric field is distributed as $E_{\mathrm{IMD}} \sim \cos^3(\pi x/L) \simeq (3/4)\cos(\pi x/L)$, ignoring the $(1/4)\cos(3\pi x/L)$ term in the trigonometric identity. It is argued that the second term can be ignored because it will not propagate in the resonator since it has the wrong wavelength for the IMD frequency. However, our results clearly show that the IMD power distribution is very poorly described by a $P_{\mathrm{IMD}} \sim |E_{\mathrm{IMD}}|^2 \sim \cos^2(\pi x/L)$ term alone (see Fig. 4), suggesting that our understanding of how IMD power is distributed in resonant systems may be incomplete.

We can simply model the intermodulation as being due to a microwave surface impedance which increases as $R_s(H_{\mathrm{rf}}) = R_s(0)(1+\alpha H_{\mathrm{rf}}^2)$, and $X_s(H_{\mathrm{rf}}) = X_s(0)(1+\beta H_{\mathrm{rf}}^2)$.[18] Assuming that the reactance nonlinearity dominates,[2] we can calculate the intermodulation levels following standard practices[14] and compare them to our measured IMD powers to determine the parameter β. The resulting values of $\beta(T/T_c) \sim 10^{-4}$ to $2\times 10^{-3}\,\mathrm{Oe}^{-2}$ for $T/T_c = 0.78$ to 0.97 are in good agreement with those obtained by Oates *et al.* from direct nonlinear surface impedance measurements on $YBa_2Cu_3O_7$ stripline resonators.[18] The fact that a quantitative weak link model was consistent with the stripline data[18] suggests a similar weak link origin for the nonlinearities observed here.

We believe that our IMD images represent the total standing wave pattern developed by the nonlinearities in the resonator, as opposed to an image of locally generated IMD. Because the nonlinearities are thought to arise from current dependence of the surface impedance, the IMD signals should start from the center of the resonator (the current antinode in the fundamental mode) and propagate outwards. We see no signal at the center of the resonator at both the fundamental and IMD frequencies, implying that the resonant IMD fields alone are being imaged.

In conclusion, using a cryogenic near-field scanning microwave microscope, we have demonstrated frequency-selective imaging of electric fields generated by nonlinearities in a superconducting microstrip resonator. The intermodulation image shows that there is a simple relationship between the linear and nonlinear power levels at each location in the device and the levels are consistent with what one expects for superconductors having a modest nonlinearity in the surface impedance. Finally, the results suggest that our understanding of the spatial distribution of intermodulation fields in resonant systems may be incomplete.

The authors wish to acknowledge assistance from S. K. Dutta, C. P. Vlahacos, and D. E. Steinhauer, as well as helpful discussions with T. Dahm, and R. B. Hammond. This work has been supported by NSF Grant No. ECS-9632811, an NSF SBIR (DMI-9710717) subcontract from Neocera, Inc., and by the Maryland Center for Superconductivity Research.

[1] T. Dahm and D. J. Scalapino, Appl. Phys. Lett. **69**, 4248 (1996).
[2] R. B. Hammond, E. R. Soares, B. A. Willemsen, T. Dahm, D. J. Scalapino, and J. R. Schrieffer, J. Appl. Phys. **84**, 5662 (1998).
[3] T. C. Sollner, J. P. Sage, and D. E. Oates, Appl. Phys. Lett. **68**, 1003 (1996).
[4] W. Diete, M. Getta, M. Hein, T. Kaiser, G. Müller, H. Piel, and H. Schlick, IEEE Trans. Appl. Supercond. **7**, 1236 (1997).
[5] M. Golosovsky, Supercond. Sci. Technol. **9**, 1 (1996).
[6] P. P. Nguyen, D. E. Oates, G. Dresselhaus, and M. S. Dresselhaus, Phys. Rev. B **48**, 6400 (1993).
[7] M. A. Hein, C. Bauer, W. Diete, S. Hensen, T. Kaiser, V. Z. Kresin, and G. Müller, J. Supercond. **10**, 485 (1997).
[8] C. Wilker, Z. Y. Shen, P. Pang, W. L. Holstein, and D. W. Face, IEEE Trans. Appl. Supercond. **5**, 1665 (1995).
[9] G. Hampel, B. Batlogg, K. Krishana, N. P. Ong, W. Prusseit, H. Kinder, and A. C. Anderson, Appl. Phys. Lett. **71**, 3904 (1997).
[10] A. S. Thanawalla, S. K. Dutta, C. P. Vlahacos, D. E. Steinhauer, B. J. Feenstra, S. M. Anlage, and F. C. Wellstood, Appl. Phys. Lett. **73**, 2491 (1998).
[11] A. S. Thanawalla, W. Hu, D. E. Steinhauer, S. K. Dutta, B. J. Feenstra, S. M. Anlage, F. C. Wellstood, and R. B. Hammond, IEEE Trans. Appl. Supercond. **9**, 3042 (1999); cond-mat/9811141.
[12] S. K. Dutta, C. P. Vlahacos, D. E. Steinhauer, A. S. Thanawalla, B. J. Feenstra, F. C. Wellstood, S. M. Anlage, and H. S. Newman, Appl. Phys. Lett. **74**, 156 (1999).
[13] Z. Y. Shen, *High-Temperature Superconducting Microwave Circuits* (Artech, Boston, 1994), p. 47.
[14] S. K. Remillard, L. J. Klemptner, J. D. Hodge, T. A. Freeman, P. A. Smith, and T. W. Button, Proc. SPIE, **2559**, 59, 1995.
[15] B. A. Willemsen, K. E. Kihlstrom, and T. Dahm, Appl. Phys. Lett. **74**, 753 (1999).
[16] The spatial resolution of the microscope is limited to the probe-sample separation (550 μm) in this case, hence the deep dip in fundamental power at the center of the resonator is not resolved in Fig. 4.
[17] O. G. Vendik, I. B. Vendik, and T. B. Samoilova, IEEE Trans. Microwave Theory Tech. **45**, 173 (1997).
[18] D. E. Oates, P. P. Nguyen, G. Dresselhaus, M. S. Dresselhaus, and C. C. Chin, IEEE Trans. Appl. Supercond. **3**, 1114 (1993).